Aalborg Universitet

AALBORG UNIVERSITY
DENMARK

Adaptive Generalized Predictive Voltage Control of a Boost Converter for Peak Current Reduction in the Presence of Uncertainties

Asvadi-Kermani, Omid; Felegari, Bashir ; Amani, Danesh; Momeni, Hamidreza ; Hajizadeh, Amin; Oshnoei, Arman

Published in:
I E E E Transactions on Industrial Informatics

Publication date:
2024

Link to publication from Aalborg University

Citation for published version (APA):
Asvadi-Kermani, O., Felegari, B., Amani, D., Momeni, H., Hajizadeh, A., & Oshnoei, A. (2024). Adaptive Generalized Predictive Voltage Control of a Boost Converter for Peak Current Reduction in the Presence of Uncertainties. *I E E E Transactions on Industrial Informatics*.

General rights
Copyright and moral rights for the publications made accessible in the public portal are retained by the authors and/or other copyright owners and it is a condition of accessing publications that users recognise and abide by the legal requirements associated with these rights.

- Users may download and print one copy of any publication from the public portal for the purpose of private study or research.
- You may not further distribute the material or use it for any profit-making activity or commercial gain
- You may freely distribute the URL identifying the publication in the public portal -

Take down policy
If you believe that this document breaches copyright please contact us at vbn@aub.aau.dk providing details, and we will remove access to the work immediately and investigate your claim.

Adaptive Generalized Predictive Voltage Control of a Boost Converter for Peak Current Reduction in the Presence of Uncertainties

Omid Asvadi-Kermani, *Graduate Student Member, IEEE,* Bashir Felegari, *Graduate Student Member, IEEE,* Danesh Amani, *Member, IEEE*, Hamidreza Momeni*, Senior Member, IEEE,* Amin Hajizadeh, *Senior Member, IEEE,* Arman Oshnoei, *Member, IEEE.*

***Abstract*— This paper introduces an adaptive constrained generalized predictive controller (GPC) applied to a float interleaved boost converter (FIBC) with a low output current. FIBCs face uncertainties due to thermal effects in switches and diodes, variable operating frequencies, inductor losses, measurement errors, and load changes. The controller uses FIBC's direct duty cycle/output voltage model. It features constraints on the control signal and its variations, helping to regulate the input peak current. The controller's stability and performance under uncertainties are enhanced by three mechanisms: adaptive adjustment of control signal's upper constraint and the output error weight coefficient, and an online model estimation mechanism for the GPC. This includes constraining estimated model poles for assured closed-loop stability. Experimental results with 20% real uncertainties and load changes demonstrate the controller's effectiveness: it reduces input peak current, and output voltage oscillations, and overshoots by 3.5A, 1V, and 7.5%, respectively, compared to a basic constrained GPC.**

***Index Terms*-- Adaptive control, float interleaved boost converter, generalized predictive controller, model uncertainties, steady-state response, transient response.**

I. Introduction

POWER electronic applications have become increasingly prevalent in improving the operation of power grids and renewable energy sources over recent decades. Numerous studies focus on enhancing the performance of these applications through the implementation of more effective controllers. Low output current float interleaved boost converters (FIBCs), a specific type of DC/DC converter, are employed to increase the output voltage of photovoltaic systems and EV battery packs. FIBCs can be seamlessly integrated with inverters and power grids. Given the low output voltages of photovoltaic systems and battery packs, there is a need to boost the DC voltage for connection to the AC inverter input. These converters are applicable in both 200V DC/110V AC single-phase and 400V DC/120V AC three-phase inverters. The converters under investigation are typically used to elevate the output voltages of parallel-connected PV cells, as detailed in [1], [2]. The proposed power electronic interface, designed for both electric and hybrid vehicles, is presented in [3], [4]. The FIBC converter is a proper option for low-voltage renewable energy sources, such as battery packs and solar panels. It comprises two conventional boost converters connected in series, which facilitates maximum voltage gain while minimizing output voltage ripples, as detailed in [3]. Typically, the FIBC converter has a higher component count compared to traditional boost converters, resulting in increased construction and implementation costs. To improve its performance, various controllers have been applied to FIBC converters, including Proportional-Integral (PI) controllers [5], nonlinear adaptive control [6], and sliding mode controllers [7]. The model predictive controller (MPC) is an optimization-based controller increasingly used in controlling power systems and industrial processes, owing to its advanced features. Recent studies have demonstrated that MPC offers good stability and is more easily implementable in real systems due to its discrete nature [8]. Additionally, MPC can be applied in a constrained form, enhancing the controller's performance and improving the closed-loop system's stability. The capability of implementing constraints in MPC also aids in achieving simulation results that more closely resemble actual system outcomes, with constraints applied to both the system output and control variables. MPC can be modified to function as either a robust or adaptive MPC controller. Various forms of adaptive MPC have been investigated in [9], [10]. Robust MPC, based on convex hull approximation, was investigated in [11]. In [12], MPC was studied for interleaved boost converters. The use of enumeration-based MPC for direct voltage control of DC/DC boost converters was explored in [13].

The developed method in [14] describes the implementation of online weighting factor optimization using simplified simulated annealing for finite set predictive control on an induction motor, enhancing its robustness.

In [15], an interleaved boost converter is managed using a dynamic neural-based Model Predictive Control (MPC) with

Omid Asvadi-Kermani,Bashir Felegari , Danesh Amani and, Hamidreza Momeni are with the Electrical Engineering Department, Tarbiat Modares University, Tehran, Iran. Corresponding author: Omid Asvadi-Kermani (emails: o.asvadikermani@modares.ac.ir, bashir.felehgari@modares.ac.ir , a.danesh@modares.ac.ir , momeni_h@modares.ac.ir). Amin Hajizadeh and, Arman Oshnoei are with Department of Energy Technology , Aalborg University , Denmark , (emails : aha@et.aau.dk, aros@et.aau.dk).

adaptive constraint tuning to improve performance against input voltage fluctuations, focusing on control signal adjustments. The complexity of the converter's average state-space model posed significant implementation challenges for the MPC controller.

The study in [16], presents an explicit model predictive control (EMPC) technique for high-frequency DC-DC converters, utilizing a backpropagation neural network (BPNN) to pre-calculate control laws, reducing online computational demands. However, adjusting to operational changes remains computationally intensive. To address this, it proposes using BPNNs to approximate control laws offline, aiming to balance control performance with reduced storage and computational needs. While focusing on a simple converter, the complexity and data requirements of the MPC method, alongside its focus on control signal limitations without assessing quality changes, are notable.

In [17], a boost converter performance is enhanced with a model predictive controller that leverages a detailed nonlinear state-space model for rigorous stability analysis and design. The method identifies the control signal directly from the cost function, which may induce oscillations, and computes this signal through a non-iterative closed formulation, simplifying the process.

In [18], a buck-boost converter operation is managed using an unconstrained generalized predictive control model that captures the system's small signal input-output behavior independently of the input current. The model's precision is vital for controller efficacy, yet it operates without constraints on the control variable, posing risks of instability during rapid system changes. Additionally, the system demonstrates low output power and voltage in testing.

In [19], a variable self-tuning horizon mechanism for generalized predictive control is introduced, applied to a simplistically designed boost converter with a single switch. While the algorithm's complexity, based on an exact state-space model, allows for precise disturbance modeling, it faces challenges in observer parameter optimization and reference variable generation. Testing focused solely on load changes, omitting startup transient response analysis. The unconstrained execution of the GPC algorithm, without control variable limitations, could threaten system stability. Despite using advanced dSpace control hardware, the demonstration lacks in showing control variable adjustments.

Two major sources of uncertainty are parametric uncertainty and input DC voltage source uncertainty. It is essential for the voltage controller to keep the output voltage close to its reference value despite these uncertainties, which may fluctuate over time due to changes in working conditions and environmental temperature. For instance, in [20], the voltage regulation of a conventional boost converter was carried out using reduced-order PI observers, taking into account both parametric and input voltage uncertainties.

The major contribution of this study is the development of a direct voltage controller for the FIBC converter utilizing two types of constrained Generalized Predictive Control (GPC) controllers. These controllers have fewer parameters compared to the typical state-space model for the FIBC. The GPC method's structure, derived from solving the Diophantine equation, is inherently more resistant to uncertainty than other methods, as noted in [21]. The proposed controller is a constrained GPC with adaptive tuning of the control variable constraint. It effectively regulates both the output voltage and the current of each inductor during transient and steady-state responses. In contrast to controllers presented in the literature review sections especially in [3], [15], [19], and [22], this controller demonstrates strong robustness against model uncertainties and does not require extensive pre-trained data for design. To ensure the stable operation of the closed-loop system, the controllers are implemented in a constrained form. An adaptive technique is developed to optimize the system response of a Generalized Predictive Control (GPC) controller by adjusting constraints and output weight, specifically for control variable changes. This includes an adaptive algorithm aimed at improving transient response and minimizing steady-state voltage fluctuations, alongside an estimation algorithm for setting the GPC controller targets within stable constraints. The strategy enhances system response after load changes and increases robustness to disturbances and uncertainties. Simplification of the GPC controller is achieved through a direct transfer function model, reducing computational complexity and smoothly adjusting input current without direct inductor current measurement. The experiments confirm the approach's effectiveness in reducing control signal and inductor current oscillations, showcasing the proposed method's practical implementation ability. The innovations addressing the three primary challenges of this research and the strategies implemented to overcome them are summarized as follows. To mitigate the overshoot in the output voltage and input current without direct measurement, a mechanism for setting the control variable limit is introduced in the context of the converter's transient response. An adaptive adjustment mechanism for the output weighting coefficient in the GPC cost function is introduced to minimize fluctuations in the output voltage and its steady-state error for 40V output. To ensure the stability of the closed-loop system and maintain optimal performance amid disturbances and uncertainties, a constrained adaptive mechanism for estimating the system's online model is proposed for use in the target GPC. All results of proposed method have been compared to the basic GPC. A summarized block diagram of main parts of this research is shown in Fig. 1.

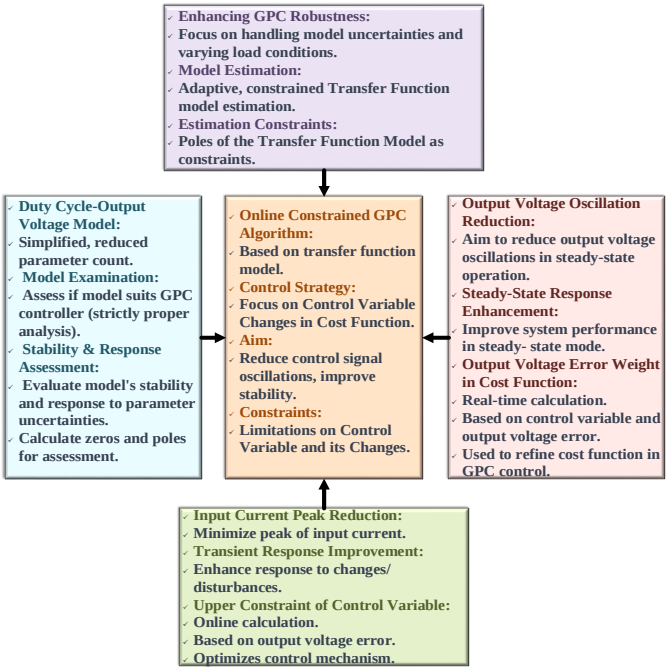

Fig. 1 Summarized block diagram of the main parts of this research

II. FIBC Model Investigation

A circuit diagram of the FIBC converter is shown in Fig. 2.

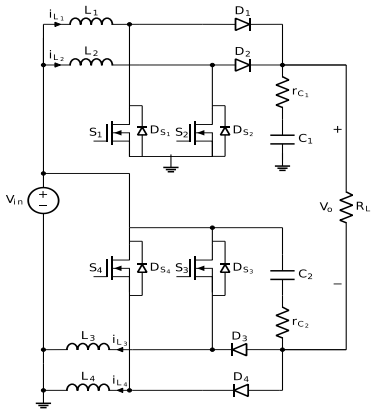

Fig. 2 Circuit diagram of the FIBC

TABLE I
EXPERIMENTAL SETUP PARAMETERS WITH UNCERTAINTIES

Component	Nominal Value	Value with Uncertainty
C_1	820 µF	(100 +820) µF , 200 V
C_2	820 µF	(100 + 50 +820) µF , 200 V
$L_{1,2}$	470 µH	330 µH
$L_{3,4}$	470 µH	570 µH
R_L	100 Ω	80 Ω (t=0.11 t=0.24 s)

The FIBC consists of two conventional boost converters connected in series. When switch S_i is off, diode D_i is on, and when S_i is in its connected mode, the diode D_i is off. D is the large signal duty cycle of FIBC and the parameter D_0 is its nominal value for each switch. d is the small signal duty cycle that has been calculated from $d = D - D_0$ [1, 23]. According to [3] the converter s' model has been investigated, here, it has been assumed that FIBC parameters are in the nominal model $L_1 = L_2 = L_3 = L_4 = L$,$r_{L_1} = r_{L_2} = r_{L_3} = r_{L_4} = r_L$, $C_1 = C_2 = C$, $r_{c_1} = r_{c_1} = r_c$. Also, R_L is output resistive load. These uncertainties in real systems may arise due to thermal effects in switches and diodes, frequency bandwidth in inductors, errors in measurement tools, uncertainty in load, and changes in environmental conditions in certain applications, such as solar panels. Small-signal transfer function models relating the duty cycle to the output voltage and the duty cycle to the inductor current are presented in equations (1) and (2) as found in [3, 23]:

$$G_v = \frac{v_o(s)}{d(s)} = K_v \frac{(1-(s/\omega_{zr}))(1+(s/\omega_{zl}))}{(1+(s/\omega_o Q)+(s^2/\omega_o^2))} \quad (1a)$$

$$G_i = \frac{I_L(s)}{d(s)} = K_i \frac{(1+s/\omega_{zi})}{(1+(s/\omega_o Q)+(s^2/\omega_o^2))} \quad (1b)$$

$$\omega_{zl} = \frac{1}{r_C C} \qquad \omega_{zi} = \frac{1}{(R_L C/(D_0+3))+r_C C} \quad (2a)$$

$$\omega_o = \frac{1}{\sqrt{LC}} \sqrt{\frac{2R_L(1-D_0)^2+2r_L}{R_L+2r_C}} \quad (2b)$$

$$Q = \frac{\omega_o(R_L+2r_C)LC}{R_L C(r_L+2r_C(1-D_0)^2)+2(L+r_C r_L C)} \quad (2c)$$

$$K_i = \frac{v_{in}(D_0+3)}{2(1-D_0)(R_L(1-D_0)^2+r_L)} \quad (2d)$$

$$K_v = \frac{v_{in}(2R_L(1-D_0)^2-r_L(1+D_0))}{(1-D_0)^2(R_L(1-D_0)^2+r_L)} \quad (2e)$$

Based on the information in Table I and the illustration in Fig. 2, the model parameters of the FBIC and the input DC voltage source are presumed to have uncertainties within a defined range. Fig. 8 displays the input DC voltage and its step changes, selected by [3] to facilitate better comparison. For the application of the GPC controller to the system, the system model must be represented as a strictly proper discrete transfer function model, as noted in [8]. According to (1), G_v is the non-minimum phase proper transfer function. After discretizing G_v and G_i transfer functions with T_s=0.001 sampling time to G_d and $G_{d,i}$ models, G_d is rewritten in (3) as follows:

$$\begin{cases} \underbrace{G_d}_{Proper} \\ G_{d,i} \end{cases} = \underbrace{G_{d,1}}_{Strictly\ Proper} + \underbrace{G_{d,2}}_{Constant\ Gain} \rightarrow \begin{cases} G_{d,2} = f_v \\ f_v \backsimeq 0.18 \end{cases} \quad (3)$$

Based on Fig. 3 and equation (3), the primary transfer function utilized in both the basic and the proposed constrained GPC controllers is $G_{d,1}$ with nominal parameter values. The system model, G_d is subject to uncertainties in its parameters and input voltage. $G_{d,2}$ exhibits a small gain in comparison to the output of the main $G_{d,1}$ model. To examine the open-loop system's poles and zeros, 1000 random discrete models Table I. Fig. 4 illustrates that within the assumed range of uncertainties, the open-loop system has two stable poles within the unit circle, indicating that the open-loop system is stable, while it has one unstable zero.

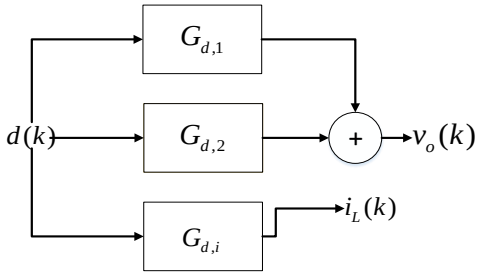

Fig. 3 FIBC discrete model block diagram

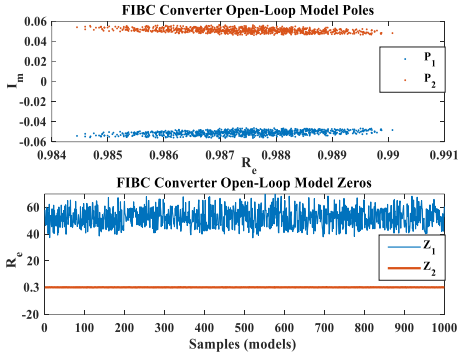

Fig. 4 Open-loop system poles and zeros for 1000 random discrete models (G_d)

In summary, this section describes the model of the direct transfer function from the small duty cycle signal to the output voltage of the converter, along with its parameters. The model's simplicity is particularly emphasized. It is then discretized using a specified sampling time. To explore the feasibility of introducing uncertainty within a specified range, the locations of the model's zeros and poles have been identified. Results indicate that among 1000 models with random uncertainty in the specified range, the model remains stable but exhibits a non-minimum phase. Consequently, for the implementation of the GPC algorithm, which requires a strictly proper model, the discrete model was divided into two parts: a strictly proper model and a small fixed gain. The transfer function parameters are utilized strictly as initial values in the adaptive estimation algorithm of the model.

III. Constrained Generalized Predictive Controller

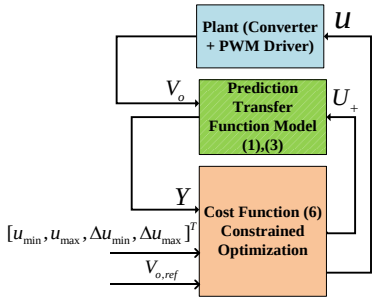

Fig. 5 Overall block diagram of the system and the basic constrained generalized predictive controller

Consequently, the system model is of a non-minimum phase type. Fig. 5 illustrates that MPC is an optimization-based control method typically employed for the system's state-space model. It has been observed that GPC demonstrates robustness against small disturbances and uncertainties, thus making it a favorable control method. A significant advantage of GPC is its ability to be implemented in a constrained manner. GPC, a transfer function-based MPC controller, is widely used in various industrial processes, as referenced in [8, 24]. Its main characteristics include: 1) utilization of the process's discrete transfer function, 2) suitability for implementation on non-minimum phase converters, delayed, and unstable systems, and 3) strong robustness against disturbances. The GPC algorithm is implemented using discrete models, with the CARIMA (Controlled Auto-Regressive Integrated Moving Average) model being employed in this study. It is important to note that the disturbance term is considered zero in this work. In general, the GPC algorithm can be expressed as:

$$A(z^{-1}) = 1 + a_1 z^{-1} + \ldots + a_{n_a} z^{-n_a}, \Delta(z^{-1}) = 1 - z^{-1} \quad (4a)$$

$$B(z^{-1}) = b_0 + b_1 z^{-1} + \ldots + b_{n_b} z^{-n_b} \quad (4b)$$

$$\underbrace{\Delta(z^{-1})A(z^{-1})y(t) = \Delta(z^{-1})z^{-dd}B(z^{-1})u(t-1)}_{CARIMA} \quad (4c)$$

Where polynomial $A(z^{-1})$ is the output dynamics and polynomials $B(z^{-1})$ and $C(z^{-1})$ are control input and disturbance dynamics. n_a, n_b , $and\ n_c$ are the degrees of these polynomials. dd is the input delay. $\Delta(z^{-1})$ is an integrator that is added to the model to zero steady-state error. The objective is to minimize cost function (J) and generate the desired control signal $u(k)$. In this paper, dd value is zero. This model is selected because there is an Integrator term (4a) in the model that helps to reduce the steady-state error of output and increase closed-loop stability [8]. The prediction output is calculated over the prediction horizon using the Diophantine equation as follows:

$$\tilde{A}(z^{-1}) = \Delta A(z^{-1}) \rightarrow 1 = E_j(z^{-1})\tilde{A}(z^{-1}) + z^{-j}F_j(z^{-1}) \quad (5a)$$

$$G_j(z^{-1}) = B(z^{-1})E_j(z^{-1}) \quad (5b)$$

(5a) is a Diophantine equation and $E_j(z^{-1})$, $F_j(z^{-1})$ are Diophantine polynomials that are calculated by the recursive equations. The cost function is specified as follows:

$$Y = \underbrace{\phi Y_- + \pi U_-}_{\text{Free Response}} + \underbrace{\Omega U_+}_{\text{Force Response}} , \underbrace{\Delta u(t) = U_+(1,1)}_{\text{receding horizon}} \quad (6a)$$

$$J = (Ref - Y)^T H (Ref - Y) + U_+^T R U_+ \quad (6b)$$

$$\Delta u_{min} < \Delta u(k) < \Delta u_{max}\ , u_{min} < u(k) < u_{max} \quad (6c)$$

Y is the estimated output vector along the prediction horizon. Ref reference signal vector and R and Q matrixes of the input and output weights are selected using the experimental results by repeating the tests. p is the prediction horizon, and m is the control horizon. $\Delta u(t)$ is the control signal variation obtained from (6). Ω،π ϕ matrixes and U_+،U_-،Y_- are defined as follows:

$$\phi = \begin{bmatrix} f_{d+1,0} & \cdots & f_{d+1,na} \\ \vdots & \ddots & \vdots \\ f_{d+p,0} & \cdots & f_{d+p,na} \end{bmatrix}, \pi = \begin{bmatrix} g_{d+1,1} & \cdots & g_{d+1,nb} \\ \vdots & \ddots & \vdots \\ g_{d+p,p} & \cdots & g_{d+p,nb} \end{bmatrix} \quad (7a)$$

$$\Omega = \begin{bmatrix} g_{d+1,0} & \cdots & 0 \\ \vdots & \ddots & \vdots \\ g_{d+p,m-1} & \cdots & g_{d+p,0} \end{bmatrix} \quad \begin{matrix} U_+ = [\Delta u(k) \cdots \Delta u(k+m-1)]^T \\ U_- = [\Delta u(k) \cdots \Delta u(k-n_b)]^T \\ Y_- = [y(k) \cdots y(k-n_a)]^T \end{matrix} \quad (7b)$$

According to [8], it is evident that the GPC method differs from conventional MPC approaches. In GPC, the discrete transfer function model of the system is initially formulated based on changes in the control variable. This model is then utilized to calculate the outputs during the prediction horizon. Subsequently, the parameters of the prediction model (as shown in (7)) are recursively determined by solving the Diophantine equation, following (5a). This inclusion of an integrator in the method enhances the control structure's ability to handle system uncertainties and increases its robustness against external disturbances. Moreover, by using the changes in the control signal as the basis for the cost function, this method ensures a smoother control signal and improved closed-loop stability, particularly when implemented in a constrained manner.

IV. Applying Proposed Controller On The System

According to [8, 21] and Section III, the GPC controller employs the system's discrete transfer function model and requires less data from the system model compared to other types of MPC controllers to achieve high control accuracy using a full state-space model. The GPC controller demonstrates satisfactory closed-loop stability and responds effectively in the presence of uncertainties. In this study, two types of constrained GPC controllers are applied to the FIBC model. These controllers are categorized as continuous control-set MPC controllers and involve an online constrained optimization process to determine the optimal control signal for each sample. To exhibit the controller's performance amidst uncertainties, the discrete model $G_{d,1}$ with the nominal parameter values of the FIBC (as listed in Table I) utilized in this section. The prediction and control horizon values are reduced to diminish the size of the matrices in (7) and to alleviate the overall computational burden.

A. Basic Constrained GPC

Controlling the currents of inductors is a crucial aspect when designing controllers for DC converters. In this paper, a direct voltage controller is applied to the duty cycle-to-output voltage transfer function model, as discussed in section II. To ensure effective control, constraints are imposed on the control signal$(D(k) \rightarrow u(k))$, considering the predicted output and the cost function (6). These constraints are designed to limit the current and its oscillation, which may affect the algorithm's control capability. The constraints are defined in equation (8) as follows:

$$-0.03 < \Delta u(k) < 0.03, 0 < u(k) < 0.65 \qquad (8)$$

This controller employs a prediction horizon and a control horizon (p, m) equal to 4. The weight matrices (R, H) of the cost function (6d) are tuned to balance the convergence speed of the output voltage $(V_o\,(k))$, steady-state error, and oscillations, as well as those of the control signal and its final value, to enhance the controller's performance. These constraints and parameters are selected through experimental tests, and repeated until the results are satisfactory and as closely aligned as possible with those of the real system.

B. Constrained GPC with Adaptive Output Weight and Constraint Tuning

1) Tuning Control Signal Constraint

The proposed control system block diagram is shown in Fig.5.

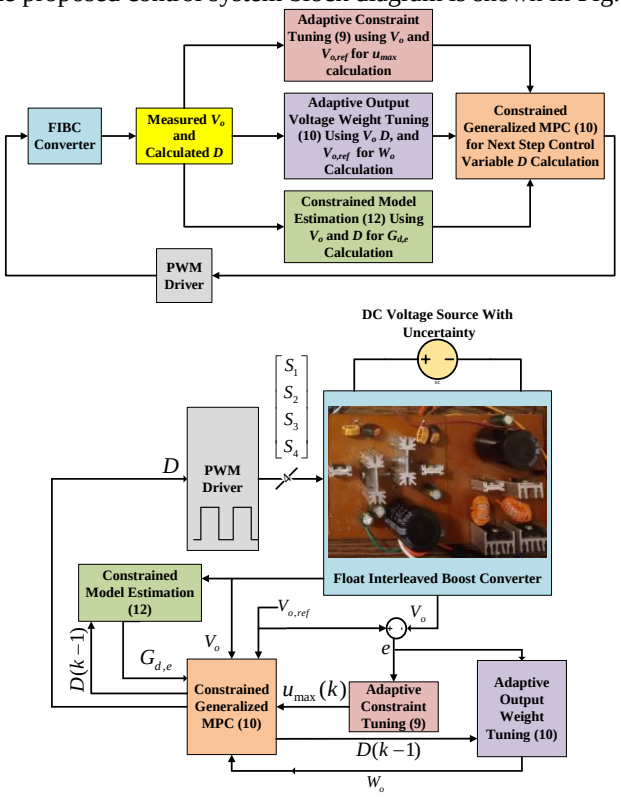

Fig. 6 The proposed control system block diagram and the proposed GPC flow diagram

In this section, the proposed GPC control algorithm and its parameters remain the same as in the previous section, except for the control signal constraint u_{max} and the output weight coefficient in the cost function, which are adaptively tuned. The primary focus of this work is on the system's transient and steady-state responses. During the transient response phase, the main objective is to eliminate output voltage overshoots while maintaining the system's response stability and reducing the initial inductor currents to expedite the transition to a steady-state. For the system's steady-state response, the aim is to minimize fluctuations in the output voltage around the reference value. The adaptive constraint tuning mechanism is detailed in equation (9):

$$\begin{cases} \alpha, \beta > 0, 1 > \varepsilon > 0.6, |\alpha e(k)| < \beta \\ e(k) = v_{ref} - v_o(k), \alpha = \dfrac{\varepsilon u_{\max,}}{40} \end{cases} \qquad (9a)$$

$$\begin{cases} if\ e(k) > 0 \rightarrow \tilde{u}_{\max}(k) = -\alpha e(k) + \beta \\ if\ e(k) < 0 \rightarrow \tilde{u}_{\max}(k) = \alpha e(k) + \beta \end{cases} \qquad (9b)$$

The value of β is selected to be close to, yet less than, $u_{max} = 0.6$. The value of α is chosen such that $\alpha e(k)$ is close to β, and their sum is a small value, aimed at reducing the initial peak current of the inductors and minimizing output voltage overshoots. Equation (9a) is used as a reference to select these parameters (α, β), with their appropriate values determined through repeated experimental tests and analysis of the results. During the transient response,$\tilde{u}_{\max}(k)$ starts very small at the beginning of the test, and $\alpha e(k)$ is positive. As the output error

decreases over time, the value of $\alpha e(k)$ increases, resulting in a gradual change in the optimizer's output signal. This gradual adjustment aids the constrained optimizer in preventing abrupt changes in output voltage and current during the transient response. If the output voltage exceeds the reference value, the sign of $\alpha e(k)$ becomes negative, assisting the optimizer in more rapidly reducing the controller output (k). In the steady-state response, due to time-varying uncertainties in the system parameters and the converter's input voltage, the converter model may vary. By adaptively adjusting the constraint, the output oscillations around the reference value and fluctuations in inductor current and control variable are reduced compared to the basic constrained GPC and robust MPC described in [3].

2) *Tuning the Output Voltage Weight in the Cost Function*

To improve the performance of the previous algorithm and address the quality of the transient and steady-state response of the output voltage under uncertainties, a mechanism featuring an adaptive weighting coefficient W_o is proposed.

This mechanism is incorporated into the cost function of the target controller, aiming to enhance smooth performance by increasing the inductor currents. The equations for this mechanism are detailed below in equation (10).

$$J = (Ref - Y)^T H (Ref - Y) + U_+^T R U_+ \tag{10a}$$

$$H = W_o W_{u,} W_o = \left| k_w \frac{u(k-1) + c_w}{y(k) - V_{o,ref}} \right| \tag{10b}$$

The weighting coefficient W_u is a unit square matrix, while k_w and c_w are constant coefficients, with $c_w$being a small fixed bias. As depicted in (10), the cost function of the target controller comprises two parts: one related to changes in the control signal and the other to the output error. The weighting coefficient of the output error enables control over its influence on minimizing the cost function. Specifically, at the start of the control algorithm's execution, during the system's transient response, the control signal is zero, and the output error is at its maximum. Consequently, the weighting coefficient of the output error W_o is at its minimum value, leading the optimization algorithm to focus on the term related to changes in the control signal, $U_+^T R U_+$. to change gradually, leading to a smooth and overshoot-free transient response in the output voltage of the converter. Additionally, it's essential for the converter's input current, namely the inductor currents, to increase steadily without significant peaks. As the control signal increases and the output error $\left(y(k) - y_{ref}\right)$ decreases, the weighting coefficient related to the output W_o also increases. This enhancement amplifies its impact on the controller's cost function. Consequently, this adjustment reduces output voltage fluctuations during steady-state responses, even with changes in load and input voltage. Unlike the basic GPC in equation (6), the cost function of the proposed controller is not exclusively dependent on the system model. The adaptive and online adjustment of the output weighting coefficient further improves system response, especially in the presence of discontinuities in converter components, particularly during changes in load and input voltage. Therefore, the proposed control structure demonstrates increased robustness. The small bias c_w is a positive value that ensures the optimizer considers the output error in the cost function optimization. The coefficient k_w influences the overall magnitude of the output weighting coefficient. These two constants are determined through repeated tests and analyses of the output voltage results to minimize output voltage error and prevent overshoot in both input current and output voltage. If these coefficients are set too low, the controller's speed may become excessively slow, potentially reducing the control signal to zero. On the other hand, if these coefficients are too high, the system might experience an overshoot in its transient response and steady-state fluctuations. Finding the appropriate values for these constants is crucial for achieving the desired performance of the system.

3) *Online Adaptive Model Estimation*

The final section of this study concentrates on the adaptive estimation of the model parameters, $G_{d,1}$, which are essential for configuring the target GPC controller. This estimation process is executed in a constrained manner, aiming to enhance the system's robustness against disturbances and uncertainties in parameters. System stability is assured by ensuring that the poles of the estimated model are maintained within the unit circle, as outlined in [21]. This method has notably improved the system's steady-state response, particularly in scenarios involving load changes. The estimated model parameters, denoted as $G_{d,e}$ are defined in accordance with (11).

$$G_{d,e}(k) = \frac{\tilde{y}(k)}{D(k)} = \frac{B_{d,e}(k) = b_0(k)z^{-1} + b_1(k)z^{-2}}{A_{d,e}(k) = 1 + a_1(k)z^{-1} + a_2(k)z^{-2}}$$
$$\theta_{d,e}(k) = [a_1(k), a_2(k), b_0(k), b_1(k)] \tag{11}$$

$$\begin{cases} J_{d,e} = (\tilde{y}(k) - V_o(k))^2 \rightarrow Argument\ \theta_{d,e} \\ P_1, P_2 \rightarrow poles\ of\ the\ G_{d,e} \\ -0.999 \leq P_1(k), P_2(k) \leq 0.999 \end{cases} \tag{12}$$

According to Fig. 5 and (12), an online constrained sequential quadratic programming (SQP) estimation algorithm using the fmincon solver in MATLAB has been employed to update the parameters $\theta_{d,e}(k)$ of the model $G_{d,e}(k)$. This estimation is performed during the execution of the proposed GPC algorithm using the output signal of the controller d and the output voltage V_o. The algorithm includes constraints on the poles of the estimated model to ensure the stability of the model. The results of this model estimation are presented in the experimental section, as shown in Fig. 11, to validate the performance of the proposed controller. To enhance the convergence of the model parameters in each iteration, the initial value $\theta_{d,e}(k-1)$ is used in the estimation algorithm for calculating $\theta_{d,e}(k)$. In summary, the proposed GPC controller consists of three main components. The first part involves the adaptive adjustment of the control signal constraint to eliminate overshoot in the converter's transient response and ensure smoothness. The second part focuses on the adaptive adjustment of the output voltage weighting coefficient in the cost function of the controller, which contributes to a smooth transient response of the converter, reduces the peak in its current response, and decreases the system's steady-state error. The third part updates the system model adaptively, particularly to enhance the system's resilience to disturbances and parameter uncertainties.

The integration of these three aspects has significantly improved the performance of the GPC controller, enabling optimal control of the converter using a straightforward control variable to output the voltage transfer function model. Experimental results that demonstrate the effectiveness of the proposed controller are showcased in Fig. 11. It should be noted that, as per equation (4) and as previously mentioned, in this research, the polynomial (z^{-1}), which relates to the modelable disturbance, is set to zero. This decision serves two purposes. Firstly, it simplifies the model and reduces the number of parameters involved. Secondly, the implementation of an online adaptive constrained model estimation algorithm equips the proposed controller with the capability to swiftly update the model parameters in response to external disturbances or changes in the system dynamics, thereby enhancing the closed-loop stability. This feature also allows for the evaluation of the proposed Generalized Predictive Control (GPC) controller's effectiveness when unmodeled changes occur in the real system.

V. Experimental Results

Based on the previously introduced FIBC converter and two constrained GPC controllers, an experimental setup has been developed to validate their performance. The nominal values of the system parameters are listed in Table I. It is acknowledged that in real systems, all parameters exhibit uncertainty. Consequently, the effectiveness of the proposed GPC controller is evaluated under these conditions. The setup is depicted in Fig. 7, with the nominal values of its parameters detailed in Table I. To test the controllers' efficacy, the real converter inductors, capacitors, and resistive load exhibit uncertainties in the 10%-20% range, as indicated in Table I. Furthermore, as stated in section II, the open-loop FIBC converter is classified as a non-minimum phase stable system. The experimental setup includes IRFP250 switches, MUR1560 diodes, HCPL3120 MOSFET drivers, and a control interface comprising an STM32F401RE Nucleo board with a W5500 Ethernet module. The control hardware utilized is a Corei7 Laptop with 12Gb of RAM.

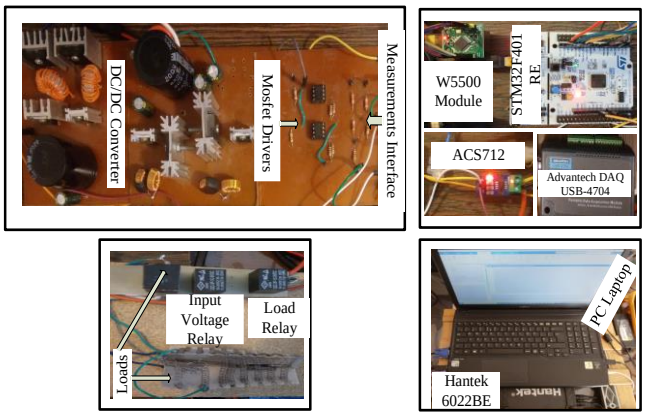

Fig. 7 Experimental setup

In this section, the parameters of the proposed constrained GPC controller were fine-tuned using the nominal values specified in Table I, alongside (8) and (9). The prediction and control horizons were set at 4. Owing to uncertainties in the experimental setup, particularly concerning the FIBC input DC voltages and load values, the output resistive load R_L was adjusted from 100 Ω to 80 Ω in the time interval from t=0.11 to t=0.24 seconds. The input DC voltage is depicted in Fig. 8. In the experimental phase, a non-ideal DC voltage source was employed to mimic more realistic operating conditions of the system. The voltage of this DC source fluctuated between approximately 9.5 V and 13 V, introducing a variable degree of uncertainty in the system's input voltage.

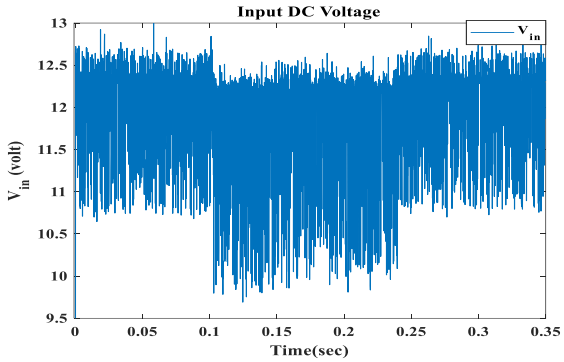

Fig. 8 Input DC voltage

This approach more effectively demonstrates the desired performance of the target controller. The experimental results, as illustrated in Figs. 9 and 10 and Table II, reveal that the constrained GPC controller with adaptive constraint tuning, when used as the direct voltage controller for a low output current FIBC, achieves a smoother transient response compared to the basic GPC. It results in smaller inductor peak currents than those observed with the basic GPC. In its steady-state response, the output voltage oscillations are maintained below 1 V for a regulated output voltage of 40 V. Furthermore, the inductors' currents and control signal exhibit smaller oscillations compared to those of the basic GPC, thereby reducing heat losses in the FIBC components, especially in the power MOSFETs. Table III provides a comprehensive comparison between this work and some prior studies. As indicated in [8, 21], GPC controllers exhibit good performance in the presence of model uncertainties and disturbances, owing to their inherent features. Moreover, the implementation of GPC controllers in a constrained manner can ensure the closed-loop stability of the system. This paper proposes two constrained GPC controllers, designed based on online optimization. Although there is no closed-form solution for closed-loop stability, the open-loop system remains stable within certain uncertainty ranges, as depicted in Fig. 4. The introduction of constraints on the control signal and its variations has markedly enhanced the closed-loop stability of the GPC controllers. Additionally, power electronics applications frequently encounter delays, such as switching-cycle delays, which are effectively modeled using non-minimum phase transfer functions. The studies [8, 21], show that the proposed constrained GPC controller responds well to non-minimum phase and delayed models in power electronics applications. The GPC, based on the system's transfer function model, is less complex compared to the steady-state model, leading to a reduced computational load. The proposed GPC

controller exhibits superior performance in managing the rapid dynamics of FIBCs. The control loop completes in just 1000 µs (sampling time). The adaptive control signal $u(k)$ constraint tuning mechanism has significantly improved the system's transient response.

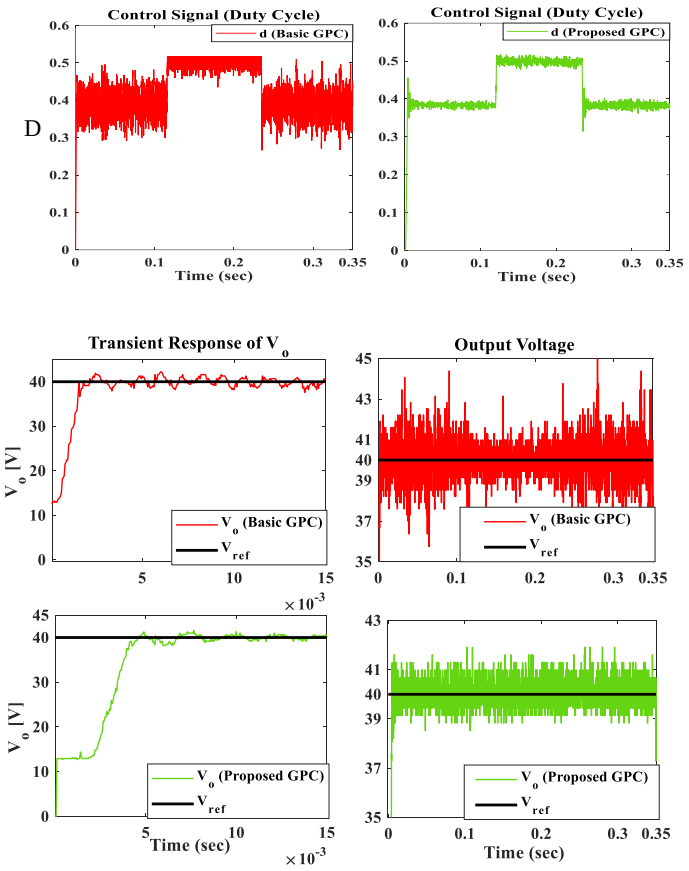

Fig. 9 Experimental results for the FIBC proposed constrained GPC for 40 volt reference (RL is the output resistive load) Output voltage both transient and steady-state responses for two GPC controllers Control signal for two GPC controllers.

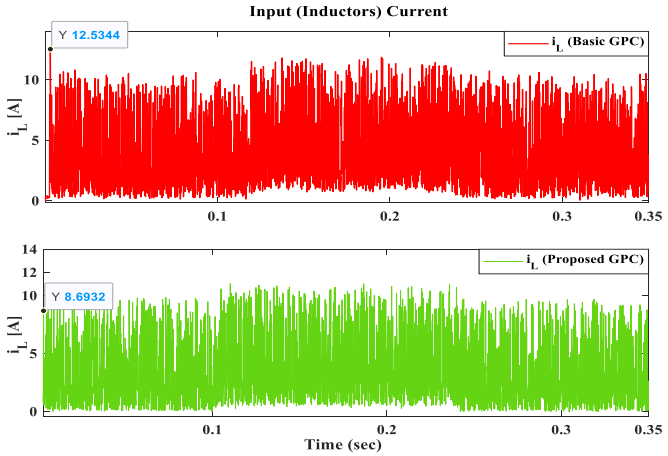

Fig. 10 Experimental results of FIBC for input inductors currents of the proposed constrained GPC voltage controller (R_L is the output resistive load) (a) basic GPC controller (b) proposed controller

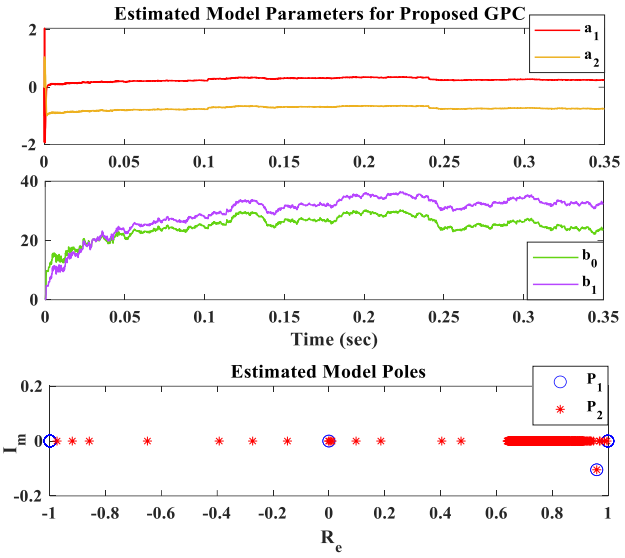

Fig. 11 Experimental results of the FIBC for input inductor currents of the proposed constrained GPC voltage controller (R_L is resistive load) that include estimated transfer function model's parameters and its poles

The convergence of the parameters associated with the output dynamics, as described in (11), is illustrated in Fig. 11. This figure shows that the parameters stabilize at a constant value after a brief period and remain largely unchanged, even with variations in the load. Meanwhile, the estimated parameters related to the input dynamics, also mentioned in (11), tend to converge to a certain range, albeit at a slower pace.

TABLE II
EXPERIMENTAL RESULTS FOR t=0 to t = 0.35 s

Parameter	Basic GPC	Proposed GPC
V_o Overshoot (%)	10%	2.5%
i_L Peak Current (A)	12.53	8.7
The sum of the absolute value of i_L	13855	13142
V_o Transient response	Aggressive	Smooth
i_L Transient response	Aggressive	Smooth
$d(k)$ response	Aggressive	Smooth
V_o Reaching Time (ms)	2.5	4
V_o Steady-state oscillation (V)	±1.5	lower than 1
Heat loss of each MOSFET (J)	6.0614	5.6303
Heat loss of each inductor (J)	4.546	4.222
SSE of output steady-state error $\sum(V_{ref} - V_o)^2$	1544	707

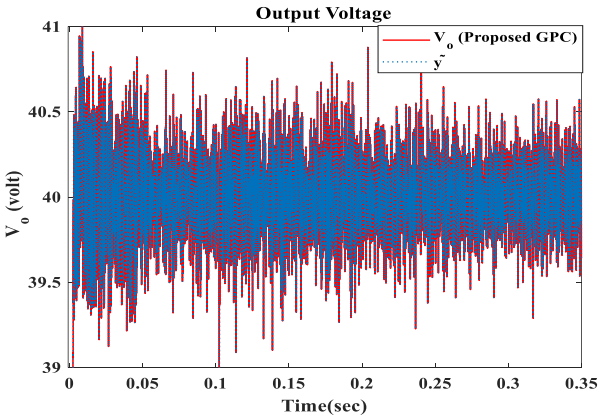

Fig. 12 Estimated model output in each step in comparison to real output voltage

Fig. 11 illustrates the variations in certain parameters when the load changes, supporting the earlier discussion about the absence of a closed-form formula for the closed-loop system when implementing the proposed GPC controller. This controller, which relies on numerical constrained optimization, ensures the stability of the closed-loop system by estimating an input-to-output transfer function model. Fig. 12 verifies that the proposed adaptive constrained GPC precisely estimates the system's transfer function model. The placement of the model's poles inside the unit circle was a key constraint for the estimator. Practical tests and calculations of the poles of the estimated model (results shown in Fig. 10) demonstrate that these poles are within the unit circle as per the constraints, confirming that the proposed adaptive constrained GPC upholds the system's closed-loop stability. The proposed GPC's response is marginally slower than the conventional GPC. This is due to the Tuning Control Signal Constraint and the adjustment of the Output Voltage Weight in the Cost Function, which are mechanisms designed to ensure a smooth transient response, thereby preventing large current peaks and excessive output voltage overshoots.

Experimental results, particularly in the low voltage range of 40 V, evaluate the performance of the proposed controller and its applicability in systems like battery charging and solar panels. In addition to the basic GPC, the proposed constrained GPC introduces several significant innovations compared to the basic method and the robust MPC developed in [3]:

1) The proposed GPC controller only requires a discrete input/output transfer function from the nominal model of the system and does not depend on primitive models with uncertainties or additional data for tuning.

2) The transfer function in the proposed GPC has fewer parameters than the state-space model used in [3], reducing computational load and making it suitable for faster systems with lower sampling frequencies.

3) An adaptive constraint and weight tuning mechanism enhances the transient response by minimizing overshoots in inductor currents and the regulated output voltage. This adaptive adjustment of constraints effectively prevents large current peaks, especially in the transient phase.

4) An adaptive model estimation mechanism improves the controller's performance in the face of uncertainties.

5) The proposed GPC's steady-state response exhibits smaller oscillations compared to the basic constrained GPC.

6) As previously mentioned, the response of the proposed GPC is slightly slower than the conventional GPC, but this is balanced by the benefits of smoother transient response and avoidance of significant current peaks and voltage overshoots (as demonstrated in Figs. 9 and 10). To clarify, as previously mentioned, there are constraints on the control variable and its changes in both the basic GPC method and the proposed controller. However, owing to the rapid dynamics of the converter and the results of the constrained optimization process in the basic method, the control signal experiences significant fluctuations. Consequently, the output voltage achieves faster convergence but exhibits overshooting and fluctuations, and the peak of the input current exceeds the recommended level. In contrast, in the proposed method, the upper limit of the control variable changes smoothly, resulting in fewer fluctuations in the control variable. This leads to reduced fluctuations and overshoot in the output voltage and a smaller peak in the input current. However, the convergence speed is slightly slower than in the basic method. In essence, a compromise has been struck between these two aspects. Nevertheless, for future research, it may be worthwhile to explore faster optimization methods to address this issue further.The experimental results for the low voltage range of 40 V validate the effectiveness of the proposed controller in practical applications like battery charging systems and solar panels.

Ultimately, it's important to acknowledge that one of the challenges with predictive control methods, particularly in constrained implementations, is the extensive computational demand. Since electronic power converters operate with rapid dynamics, the sampling time must be short. This necessitates completing control loop calculations within a very brief period. Future research could explore various constrained optimization algorithms to minimize both the time and volume of these calculations as much as possible. Fortunately, technological advancements have led to the development of affordable boards equipped with powerful processors capable of executing these methods. Additionally, in this research, efforts were made to minimize the prediction and control horizons and to employ a simple model in the controller to further this aim.

TABLE III
COMPARISON BETWEEN THIS WORK AND PREVIOUS WORKS

Ref	Control Method	Dynamic Complexity	Voltage Tracking	Robustness
[25]	IMC	High	Good	Good
[26]	MPC	High	Very Good	Good
[27]	NMPC	High	Very Good	Good
[28]	MPC	High	Good	Good
Proposed GPC	GPC	Medium	Very Good	Very Good

VI. CONCLUSION

This study focuses on improving the efficiency of DC/DC converters, which are vital components in power grid systems, by utilizing more effective control strategies. The transfer functions relating the FIBC converter's duty cycle to the output voltage and the duty cycle to the inductor current, including their uncertainties within specified ranges, have been thoroughly examined. To manage the system model as direct voltage controllers, both basic GPC and constrained GPC with adaptive control variable constraint tuning were implemented. The proposed controller is designed to ensure a smooth increase in the output voltage without any overshoots, while significantly reducing the inductor peak currents compared to the results achieved with the basic GPC. Additionally, the introduction of adaptive online model estimation has enhanced the closed-loop stability and robustness of the controller. In the proposed GPC the experimental results for transient and steady-state responses under 20% real uncertainties and load changes demonstrate that, in comparison with the basic constrained GPC, the input peak current, output voltage oscillations, and overshoot are 3.5A, 1V, and 7.5%, respectively less than the basic GPC. To alleviate the computational load, a controller designed for the transfer function model, which employs a smaller prediction and control horizon, has been utilized. The

effective implementation of this proposed controller represents a promising method for enhancing the performance of DC/DC converters. For future research, it may be worthwhile to explore fast constrained optimization methods to solve the optimization problem in the MPC. Other adaptive MPC methods can be investigated. Also, neural network data-driven models may be an interesting approach for modeling the DC converters. Other implementation configurations of MPC like distributed MPC for the converters with several switches and working modes can be helpful to increase their performance.

REFERENCES

[1] M. Kabalo, D. Paire, B. Blunier, D. Bouquain, M. G. Simões, and A. Miraoui, "Experimental validation of high-voltage-ratio low-input-current-ripple converters for hybrid fuel cell supercapacitor systems," *IEEE Transactions on Vehicular Technology*, vol. 61, no. 8, pp. 3430-3440, 2012.

[2] S. Zhuo, A. Gaillard, D. Paire, E. Breaz, and F. Gao, "Design and control of a floating interleaved boost dc-dc converter for fuel cell applications," in *IECON 2018-44th Annual Conference of the IEEE Industrial Electronics Society*, 2018: IEEE, pp. 2026-2031.

[3] H. Sartipizadeh, F. Harirchi, M. Babakmehr, and P. Dehghanian, "Robust Model Predictive Control of DC-DC Floating Interleaved Boost Converter With Multiple Uncertainties," *IEEE Transactions on Energy Conversion*, vol. 36, no. 2, pp. 1403-1412, 2021.

[4] F. Wu, W. Liu, K. Wang, and G. Wang, "Modeling and Closed-Loop Control of Three-Port Isolated Current-Fed Resonant DC-DC Converter," *IEEE Transactions on Transportation Electrification*, 2022.

[5] C. D. Lute, M. G. Simões, D. I. Brandão, A. Al Durra, and S. Muyeen, "Development of a four phase floating interleaved boost converter for photovoltaic systems," in *2014 IEEE Energy Conversion Congress and Exposition (ECCE)*, 2014: IEEE, pp. 1895-1902.

[6] H. El Fadil, F. Giri, J. M. Guerrero, and B. Salhi, "Adaptive control of interleaved boost converter for fuel cell energy," in *Proceedings of the 2011 American Control Conference*, 2011: IEEE, pp. 3905-3910.

[7] X. Hao, I. Salhi, S. Laghrouche, Y. A. Amirat, and A. Djerdir, "Backstepping Super-Twisting control of Four-Phase Interleaved Boost Converter for PEM Fuel Cell," *IEEE Transactions on Power Electronics*, 2022.

[8] E. F. Camacho and C. B. Alba, *Model predictive control*. Springer science & business media, 2013.

[9] T. A. N. Heirung, B. E. Ydstie, and B. Foss, "Dual adaptive model predictive control," *Automatica*, vol. 80, pp. 340-348, 2017.

[10] M. Tanaskovic, L. Fagiano, and V. Gligorovski, "Adaptive model predictive control for linear time varying MIMO systems," *Automatica*, vol. 105, pp. 237-245, 2019.

[11] H. Sartipizadeh and T. L. Vincent, "A new robust MPC using an approximate convex hull," *Automatica*, vol. 92, pp. 115-122, 2018.

[12] Y. Liang, Z. Liang, D. Zhao, Y. Huangfu, L. Guo, and B. Zhao, "Model predictive control of interleaved dc-dc boost converter with current compensation," in *2019 IEEE International Conference on Industrial Technology (ICIT)*, 2019: IEEE, pp. 1701-1706.

[13] P. Karamanakos, T. Geyer, and S. Manias, "Direct voltage control of DC–DC boost converters using enumeration-based model predictive control," *IEEE transactions on power electronics*, vol. 29, no. 2, pp. 968-978, 2013.

[14] S. A. Davari, V. Nekoukar, C. Garcia, and J. Rodriguez, "Online weighting factor optimization by simplified simulated annealing for finite set predictive control," *IEEE Transactions on Industrial Informatics*, vol. 17, no. 1, pp. 31-40, 2020.

[15] O. Asvadi-Kermani, B. Felegari, H. Momeni, S. A. Davari, and J. Rodriguez, "Dynamic Neural-based Model Predictive Voltage Controller for an Interleaved Boost Converter with Adaptive Constraint Tuning," *IEEE Transactions on Industrial Electronics*, pp. 1-12, 2023, doi: 10.1109/TIE.2023.3234138.

[16] J. Chen, Y. Chen, L. Tong, L. Peng, and Y. Kang, "A backpropagation neural network-based explicit model predictive control for DC–DC converters with high switching frequency," *IEEE Journal of Emerging and Selected Topics in Power Electronics*, vol. 8, no. 3, pp. 2124-2142, 2020.

[17] A. Garcés-Ruiz, S. Riffo, C. González-Castaño, and C. Restrepo, "Model Predictive Control with Stability Guarantee for Second-Order DC/DC Converters," *IEEE Transactions on Industrial Electronics*, 2023.

[18] S. M. Ghamari, F. Khavari, H. Molaee, and P. Wheeler, "Generalised model predictive controller design for A DC–DC non-inverting buck–boost converter optimised with a novel identification technique," *IET Power Electronics*, vol. 15, no. 13, pp. 1350-1364, 2022.

[19] C. Zhang, M. Li, L. Zhou, C. Cui, and L. Xu, "A Variable Self-Tuning Horizon Mechanism for Generalized Dynamic Predictive Control on DC/DC Boost Converters Feeding CPLs," *IEEE Journal of Emerging and Selected Topics in Power Electronics*, vol. 11, no. 2, pp. 1650-1660, 2022.

[20] I. H. Kim and Y. I. Son, "Regulation of a DC/DC boost converter under parametric uncertainty and input voltage variation using nested reduced-order PI observers," *IEEE Transactions on Industrial Electronics*, vol. 64, no. 1, pp. 552-562, 2016.

[21] O. Asvadi-Kermani, B. Felegari, and H. Momeni, "Adaptive constrained generalized predictive controller for the PMSM speed servo system to reduce the effect of different load torques," *e-Prime-Advances in Electrical Engineering, Electronics and Energy*, vol. 2, p. 100032, 2022.

[22] H. Sartipizadeh and F. Harirchi, "Robust model predictive control of DC-DC floating interleaved boost converter under uncertainty," in *2017 Ninth Annual IEEE Green Technologies Conference (GreenTech)*, 2017: IEEE, pp. 320-327.

[23] M. Kabalo, B. Blunier, D. Bouquain, M. G. Simões, and A. Miraoui, "Modeling and control of 4-phase floating interleaving boost converter," in *IECON 2011-37th Annual Conference of the IEEE Industrial Electronics Society*, 2011: IEEE, pp. 3026-3032.

[24] L. Wang, *Model predictive control system design and implementation using MATLAB®*. Springer Science & Business Media, 2009.

[25] X. Zhang, B. Wang, X. Tan, H. B. Gooi, H. H.-C. Iu, and T. Fernando, "Deadbeat control for single-inductor multiple-output DC–DC converter with effectively reduced cross regulation," *IEEE Journal of Emerging and Selected Topics in Power Electronics*, vol. 8, no. 4, pp. 3372-3381, 2019.

[26] M. Siami, D. A. Khaburi, and J. Rodriguez, "Simplified finite control set-model predictive control for matrix converter-fed PMSM drives," *IEEE Transactions on Power Electronics*, vol. 33, no. 3, pp. 2438-2446, 2017.

[27] X. Li, Y. Liu, and Y. Xue, "Four-switch buck–boost converter based on model predictive control with smooth mode transition capability," *IEEE Transactions on Industrial Electronics*, vol. 68, no. 10, pp. 9058-9069, 2020.

[28] C. Restrepo, G. Garcia, F. Flores-Bahamonde, D. Murillo-Yarce, J. I. Guzman, and M. Rivera, "Current control of the coupled-inductor buck–boost DC–DC switching converter using a model predictive control approach," *IEEE Journal of Emerging and Selected Topics in Power Electronics*, vol. 8, no. 4, pp. 3348-3360, 2020.

Omid Asvadi-Kermani (Gradutate Student Member, IEEE) received the B.Sc. degree in control engineering from the University of Tabriz, Tabriz, Iran, in 2018 and the M.Sc. degree in control systems engineering from Tarbiat Modares University, Tehran, Iran, in 2021., His research interests include artificial intelligence-based adaptive and predictive control in power electronics include DC/DC converters, power converters and, electrical drives, industrial electronics.

Bashir Felegari (Gradutate Student Member, IEEE) received the B.Sc. degree in power electrical engineering from Razi University, Kermanshah, Iran, in 2018, and the M.Sc. degree in control systems engineering from Tarbiat Modares University, Tehran, Iran in 2021.,He is currently a Research Assistant in microgrid control with the Laboratory of Industrial Automation and Precision Instruments, Tarbiat Modares University. His research interests include adaptive control, predictive control, power system, power electronics, and artificial intelligence

Danesh Amani (Member, IEEE) M.Sc. in Power Electronics Engineering at Tarbiat Modares University, Tehran, Iran, in 2021. His current research interests include DC-DC converters and their control techniques, quasi-resonant and resonant converters, and soft-switching techniques. He was the recipient of the best M.Sc. thesis prize in power electronics engineering by the power electronics society of Iran in 2022, and also received the best M.Sc. thesis award from the IEEE Iran Section in 2024. and PV-based renewable energy systems.

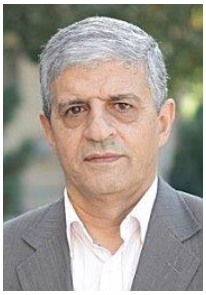

Hamidreza Momeni (Senior Member, IEEE) was born in Khomain, Iran, in 1954. He received the B. Sc. degree from Sharif University of Technology, Tehran, Iran, in 1977, the M.Sc. degree from the University of Wisconsin at Madison, Madison, WI, USA, in 1979 and the Ph.D. degree from the Imperial College of London, London, U.K., in 1987, respectively, all in electrical engineering.,He is currently a Professor with the Department of Electrical Engineering, University of Tarbiat Modares, Tehran. His research interests included Adaptive control, robust control, Fractional systems, Teleoperation systems, Industrial control, Instrumentation, Automation.

Amin Hajizadeh (Senior Member, IEEE) received the B.S. degree from Ferdowsi University, Mashad, Iran, in 2002, and the M.Sc. (Hon.) and Ph.D. (Hon.) degrees from K. N. Toosi University of Technology, Tehran, Iran, in 2005 and 2010, respectively, all in electrical engineering. In 2009, he was a guest Ph.D. Student with the Department of Electrical Power Engineering, Norwegian University of Science and Technology, Trondheim, Norway.,He was an Assistant Professor with the Shahrood University of Technology, Shahrood, Iran, from 2010 to 2014. Then, he held a postdoctoral position with the Norwegian University of Science and Technology, Trondheim, Norway, from 2015 to 2016. Since 2016, he has been an Associate Professor with the Department of Energy Technology, Aalborg University. His current research interests include control of distributed energy resources, design and control of power electronic converters for microgrid, and marine power systems.

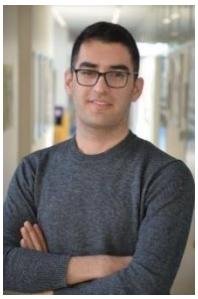

Arman Oshnoei (Member, IEEE) received the M.S. degree in electrical engineering from the University of Tabriz, Tabriz, Iran, in 2017, and the Ph.D. degree in electrical engineering from Shahid Beheshti University, Tehran, Iran, in 2021. From November 2020 to May 2021, he was a Visiting Ph.D. Scholar with the Department of Energy, Aalborg University, Aalborg, Denmark. From August 2021 to March 2022, he was a Research Assistant with Aalborg University. From May 2022 to October 2023, he was a Post-Doctoral Research Fellow with Aalborg University. He is currently an Assistant Professor of electrical power engineering with Aalborg University. His current research interests include the control and stability of power electronic-based power systems, energy storage systems, and intelligent control. He has been selected and awarded by the National Elite Foundation of Iran in 2019. He was a recipient of the Outstanding Researcher Award from Shahid Beheshti University in 2022.